

X-ray diffraction studies of trilayer oscillations in the preferred thickness of In films on Si(111)A. Gray,^{1,2} Y. Liu,³ Hawoong Hong,³ and T.-C. Chiang^{1,2}¹*Department of Physics, University of Illinois at Urbana-Champaign, 1110 West Green Street, Urbana, Illinois 61801-3080, USA*²*Frederick Seitz Materials Research Laboratory, University of Illinois at Urbana-Champaign, 104 South Goodwin Avenue, Urbana, Illinois 61801-2902, USA*³*Advanced Photon Source, Argonne National Laboratory, 9700 South Cass Avenue, Argonne, Illinois 60439, USA*

(Received 12 September 2012; published 9 May 2013)

We report a surface x-ray diffraction study of the structure of In films grown on Si(111)-(7 × 7) and Si(111)-(√3 × √3)-In substrates at a low temperature (135 K). The (7 × 7) reconstruction of the clean Si(111) surface is found to persist upon burial by the In. X-ray reflectivity measurements yield patterns that deviate strongly from the ideal case; the results suggest a complex In film structure, possibly distorted by the corrugated interfacial reconstruction. By contrast, In films grown on the Si(111)-(√3 × √3)-In surface exhibit reflectivity data that are much closer to the ideal case. The films are found to grow approximately layer by layer, resulting in a relatively small roughness. Upon annealing, the films develop preferred thicknesses at 10, 13, and 16 monolayers (MLs). Previous photoemission studies revealed preferred thicknesses at 4 and 7 MLs. Putting these results together, the preferred thickness sequence, 4, 7, 10, 13, and 16 ML, establishes a trilayer oscillation period. This period is expected from the known electronic structure of In, and arises from quantum confinement of the In valence electrons. This is the second example, after the well-known bilayer period in Pb, which shows quantum oscillations over a wide range of film thickness.

DOI: [10.1103/PhysRevB.87.195415](https://doi.org/10.1103/PhysRevB.87.195415)

PACS number(s): 68.65.Fg, 68.35.Md, 68.55.jd

I. INTRODUCTION

The confinement of electrons in metal films by a substrate at the interface and the vacuum at the surface results in quantum well states or subbands. The details are determined by the kinematics of the electrons in the film, the film thickness, and the potential barriers at the film boundaries. The quantum-well subband structure varies rapidly as a function of film thickness, which can lead to drastic differences in the properties of these films as compared to their bulk counterparts. These differences are known as quantum size effects (QSEs), and they generally exhibit a damped oscillatory behavior as a function of film thickness.¹ The damping ensures that the physical properties approach the bulk limit at large film thicknesses, and the oscillation period is given by one-half of the Fermi wavelength along the direction of the film thickness. This general behavior can be well explained by a one-dimensional shell model, in which periodic crossings of the Fermi level by the quantum-well subbands as a function of film thickness drive the damped oscillations.

A well-studied case is Pb films grown on Si(111), where a pronounced bilayer oscillation has been observed in measurements of various physical properties including the work function, stability, preferred or magic heights, and superconducting transition temperature.²⁻⁸ The bilayer oscillation period leads to an easily detected even-odd contrast for different layer thicknesses, and the data are generally well explained by models or calculations. No other systems have been studied to the same level of detail, partly because not many metal-semiconductor interfaces are chemically inert to support a well-structured quantum well system. Yet it is very desirable to examine QSEs in other materials, especially cases with a different Fermi wavelength and thus a different oscillation period. In the present work, we study the growth and annealing behavior of In films on Si(111), for which an

oscillation period of approximately 3 MLs is expected based on the known band structure of In.⁹

The growth of In films on Si(111) has been examined by a number of authors.⁹⁻¹⁵ For example, films grown on a Si(111)-(6 × 6)-Au surface showed subtle features in the electrical mean free path at 3, 6, and 9 ML thicknesses, which was interpreted in terms of roughness oscillations in the films.¹² An STM study of In films grown on Si(111)-(√3 × √3)-Pb has shown a preference for 4-ML islands at low temperatures.¹⁵ Yet other studies have reported layer-by-layer growth beyond 7 ML.^{12,13} In a recent photoemission study of In films grown on Si(111)-(√3 × √3)-In, a preference for 4- and 7-ML thicknesses was reported,⁹ in agreement with, but insufficient to prove, a trilayer period. In the present study we grew In films on the clean Si(111)-(7 × 7) surface and the Si(111)-(√3 × √3)-In surface at a low temperature (135 K) and then thermally annealed the films. For simplicity, we shall refer to these two starting surfaces simply as 7 × 7 and root-3, respectively. Surface x-ray diffraction is carried out to determine the morphology and the preferred film thicknesses, which should correspond to the local surface energy minima. For In films grown on the root-3 surface, we found preferred thicknesses of 10 and 13 ML and a hint of another preferred thickness at 16 ML. Thus 4, 7, 10, 13, and 16 ML are preferred thicknesses based on the present x-ray data and the earlier photoemission data. This sequence is sufficiently long to unambiguously confirm a trilayer period in the energetics of the system. For In films grown on the 7 × 7 surface, the 7 × 7 reconstruction remains strong after the surface is buried by In. While the data indicate a fairly smooth growth, the results could not be satisfactorily fit despite repeated efforts using a number of models, presumably because of structural distortion caused by the 7 × 7 reconstruction.

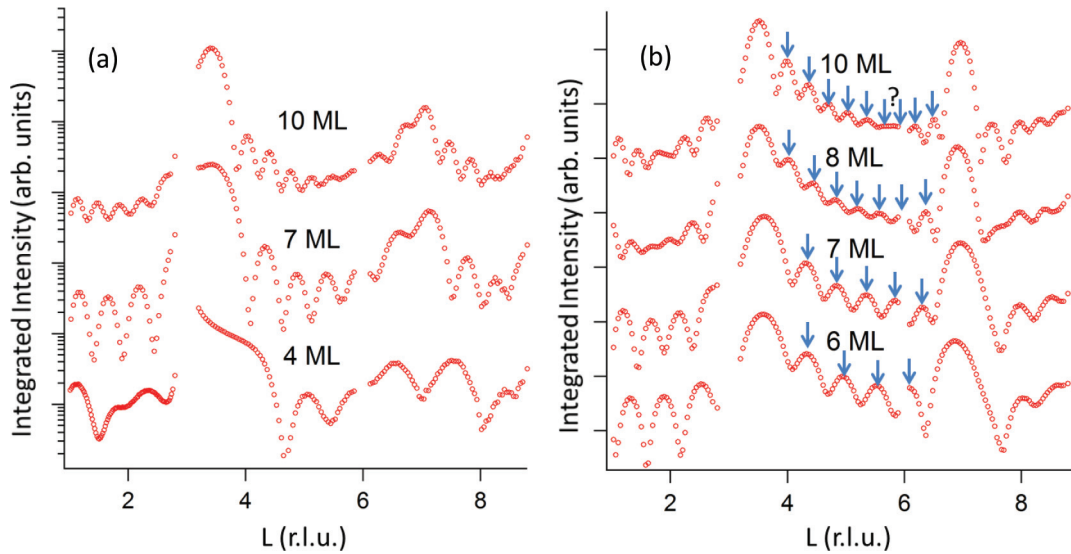


FIG. 1. (Color online) (a) Log plot of the reflectivity taken from In films grown on the 7×7 surface at 135 K. The amount of deposited In is indicated for each curve. (b) Same as (a) but for growth on the root-3 surface. The fringes are marked by arrows. The question mark indicates an uncertainty in peak identification.

II. EXPERIMENTAL DETAILS

Our x-ray diffraction experiment was performed at Sector 33-ID-E, Advanced Photon Source, Argonne National Laboratory. A 40×10 mm rectangle was cut from a commercial P-doped Si(111) wafer. The sample was mounted on a liquid nitrogen cooled manipulator, and thermally anchored to the manipulator by a sapphire block. Two thermocouples placed near each end of the sample were used to measure the sample temperature. Tantalum foils wrapped around each end of the sample provided electrical contacts for heating by running current directly through the sample. The sample could also be heated indirectly by a tungsten coil heater placed behind the sample. Each sample was outgassed for a few hours and then briefly annealed to about 1200°C , to create a clean 7×7 surface. To produce the root-3 surface, approximately 2 ML of In was deposited on the surface followed by annealing at 450°C for a few minutes. The annealing desorbs excessive indium atoms and yields a clean root-3 surface. The quality of the surfaces was verified by reflection high energy electron diffraction (RHEED) and the annealing time for the root-3 surface was adjusted so that there was no trace of $\text{Si-(111)-(4 \times 1)-In}$ or $\text{Si(111)-(\sqrt{3}1 \times \sqrt{3}1)-In}$ present in the RHEED pattern. For film growth, the deposition rate of In was set to 0.75ML/min with the substrate temperature held at around 135 K, the base temperature of the system. Data at different thicknesses were taken from the same sample with incrementally added In. After reaching a certain thickness, the films were annealed as needed to allow the system to evolve according to the energetics of the system; the sample was allowed to cool down to the base temperature before each x-ray scan.

The x-ray measurements were performed using 19.9 keV x rays and a Pilatus area detector. Two-dimensional x-ray images were taken as a function of the incident angle of the x-ray beam from which the reflectivity as a function of perpendicular momentum transfer was extracted. The background

intensity was interpolated from two strips above and below the specular position for background subtraction. Corrections were taken to account for changes in scattering geometry. A hexagonal $(HKL)_{\text{hex}}$ surface coordinate system for the Si(111) surface is used to describe the x-ray diffraction results. Details of this coordinate system can be found elsewhere.¹⁶

III. RESULTS

Figures 1(a) and 1(b) show reflectivity data for several coverages of In films grown on the 7×7 and root-3 surfaces, respectively, as a function of the perpendicular momentum transfer L in Si(111) reciprocal lattice units. Gaps in the data around $L = 3, 6,$ and 9 are to avoid the intense Si substrate peaks that could damage the detector. Broad peaks near $L = 3.5$ and 7 are at the expected In bulk Bragg peak positions. Several interference fringes can be found between these peaks which result from the layering of the In film. For an ideal freestanding and smooth film, the fringes should be equally spaced and their number should equal the number of atomic layers minus 2. The overall fringe structure should resemble a multislit interference pattern. This is approximately true for the films grown on the root-3 surface, as indicated by the downward arrows in Fig. 1(b). On close inspection, the fringe peaks are not exactly equally spaced, and the number of peaks is uncertain or off by one in some cases. This is related to structural relaxation and roughness in the film. The general trend suggests that the growth is approximately layer by layer.

By contrast, the fringe structure for the films grown on the 7×7 surface, shown in Fig. 1(a), deviates substantially from the ideal multislit interference pattern. Specifically, the In Bragg peak at $L = 7$ is not well developed, and the peak at $L = 3.5$ has a strange shape at 4 ML. These observations suggest structural complexity. Figure 2 shows two scans along momentum transfer $(H, K, L) = (0, K, 0.25)$, with K ranging from 0.9 to 1.4. One scan is for a 7-ML In film, and the other

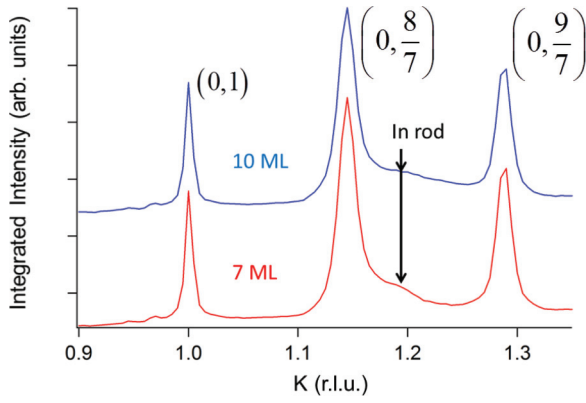


FIG. 2. (Color online) X-ray intensity as a function of K for $H = 0$ and $L = 0.25$, taken for In films of coverages of 7 and 10 ML grown on a 7×7 surface. Peaks from the 7×7 reconstruction are indicated. A peak arising from the In truncation rod is also indicated.

a 10-ML film. These scans are parallel to the sample surface and the peak at $K = 1$ corresponds to the $(0, 1)$ bulk truncation rod of Si(111). The two peaks at $K = 8/7$ and $9/7$ arise from the 7×7 reconstruction of Si(111) that remains under the In film. Also evident is a very weak peak corresponding to an In-derived truncation rod, as indicated in the figure. The 7×7 reconstruction of the clean Si(111) surface involves dimers, adatoms, and stacking faults. We do not know *a priori* which structural features are preserved or modified under the In film, and the film structure itself could be ruffled because of the corrugations associated with the 7×7 reconstruction. This is likely the reason for the more complex fringe pattern seen in Fig. 1. It is likely for the same reason that we have not been able to fit the data satisfactorily. We will focus below on the data for growth on the root-3 surface.

Figure 3 shows the reflectivity of a 10-ML film deposited on the root-3 surface at 135 K. After annealing to 210 and then 240 K, it develops more fringes in-between the In Bragg peaks.

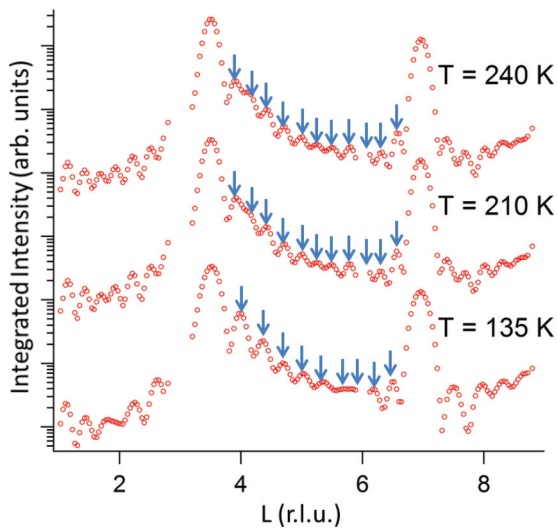


FIG. 3. (Color online) Log plot of the reflectivity taken from a 10-ML In film grown on a root-3 surface at 135 K, and after the same film has been annealed to 210 and 240 K. The fringes are marked with arrows.

Thus the film develops larger thicknesses. Heating allows the In atoms to migrate and the film to ripen in accordance with the energetics. Energetically unfavorable thicknesses are expected to diminish, and energetically preferred thicknesses are expected to grow. The change in fringe pattern can be simply interpreted in terms of roughness development in accordance with the energetics. According to Ref. 15, a phase transition from fcc(111) to bct(101) could occur at ~ 250 K and/or layer coverage above 5 ML. We did not observe such a transition in our films. The difference could be attributed to a different sample preparation scheme [note that the films in Ref. 15 are grown on a Pb terminated Si(111) substrate and at higher substrate temperatures].

IV. ANALYSIS AND DISCUSSION

The data for the films grown on the root-3 surface are analyzed in the usual manner.^{17–20} The film is modeled by domains or islands of varying thicknesses with a small portion of the substrate surface left uncovered (due to step bunches or defects). If the domains are separated by distances greater than the coherence length of the x rays the scattering intensities from the domains will add incoherently, and vice versa:

$$I(q_z) = \Lambda I_{\text{coh}}(q_z) + (1 - \Lambda) I_{\text{incoh}}(q_z), \quad (1)$$

where q_z is the perpendicular momentum transfer and I_{coh} and I_{incoh} are the coherent and incoherent fractions; these are combined by a coherence factor Λ . The coherent part of the intensity is given by

$$I_{\text{coh}}(q_z) = |A_{\text{In}}(q_z) + A_{\text{sub}}(q_z)|^2, \quad (2)$$

where $A_{\text{In}}(q_z)$ is the scattering amplitude of the In film and $A_{\text{sub}}(q_z)$ is that of the substrate. The scattering amplitude from the Si bulk substrate is given by

$$A_{\text{Si}}(q_z) \propto f_{\text{Si}}(q_z) e^{-M_{\text{Si}}} \frac{1 + e^{-iq_z a_{\text{Si}} \sqrt{3}/12}}{1 - e^{-iq_z a_{\text{Si}} \sqrt{3}/3}}, \quad (3)$$

where $f_{\text{Si}}(q_z)$ is the atomic scattering factor of Si, $e^{-M_{\text{Si}}}$ is the Debye-Waller factor, and a_{Si} is the lattice constant of Si. It is necessary in the fitting to include an interface layer of In,

$$A_{\text{sub}}(q_z) \propto f_{\text{In}}(q_z) e^{-M_{\text{In}}} \rho_{\text{int}} e^{iq_z d} + A_{\text{Si}}(q_z), \quad (4)$$

where ρ_{int} is the relative density of the interface layer and d is the distance between the last layer of Si and the interface layer. The scattering factor of the In film atop is given by

$$A_{\text{In}}(q_z) \propto \left(\frac{a_{\text{Si}}}{a_{\text{In}}} \right)^2 f_{\text{In}}(q_z) e^{-M_{\text{In}}} \sum_{N=1}^{N_{\text{max}}} p_N \sum_{j=1}^N e^{iq_z z_{j,N}}, \quad (5)$$

where the first sum adds the intensities from all possible domain thicknesses present in the film and the second sum adds the intensities from each layer in a film of thickness N . The variable $z_{j,N}$ indicates the position of layer j in a region of thickness N relative to the Si substrate surface. The variable p_N is the fraction of the surface covered by a film that is N layers thick and p_0 is the fraction of the surface not covered by the film so that

$$\sum_{N=0}^{N_{\text{max}}} p_N = 1. \quad (6)$$

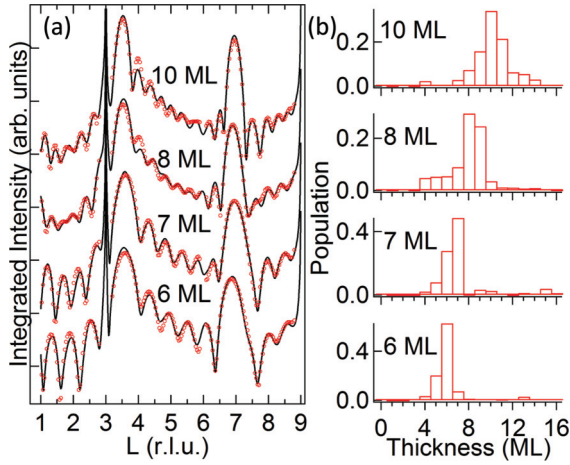


FIG. 4. (Color online) (a) Log plot of the reflectivity (red circles) taken for several different coverages of In deposited on a root-3 surface at 135 K. The black curves are fits. (b) The corresponding thickness distributions.

The average thickness of the domains present in the film is given by

$$\Theta = \sum_{N=1}^{N_{\max}} p_N N. \quad (7)$$

The incoherent part of the intensity is given by

$$I_{\text{incoh}}(q_z) = \sum_{N=1}^{N_{\max}} \frac{p_N}{1-p_0} |A_{\text{In}}^N(q_z) + A_{\text{sub}}(q_z)|^2, \quad (8)$$

where $A_{\text{In}}^N(q_z)$, the scattering amplitude from an island of thickness N layers, is given by

$$A_{\text{In}}^N(q_z) = f_{\text{In}}(q_z) e^{-M_{\text{In}}} (1-p_0) \sum_{j=1}^N e^{i q_z z_{j,N}}, \quad (9)$$

so that the intensity from each island is simply added together.

These formulas are used to fit the data. The coherence factor, the Debye-Waller factor, the individual domain occupancies, and the interatomic layer spacings were allowed to vary. A physical constraint is applied: only the layer spacings between the substrate and the first layer, the first layer and the second, the $(N-2)$ th layer and the $(N-1)$ th, and the $(N-1)$ th layer and the N th are allowed to vary independently, while the spacings for the middle layers are assumed to be the same.

The results of the fitting are shown in Fig. 4 for various amounts of In deposition at the base temperature of 135 K and in Fig. 5 for a 10-ML film after deposition and then annealing to 210 and 240 K. These data are fit simultaneously using the same set of parameters. The initial fitting parameters were chosen using reasonable guesses. The results of the fitting are shown as solid curves in Figs. 4(a) and 5(a) for the two sets of reflectivity data. Shown in Figs. 4(b) and 5(b) are the corresponding final population distributions for the various domain thicknesses.

V. DISCUSSION

The results in Fig. 4 show that each film deposited at the base temperature of 135 K has a fairly narrow thickness

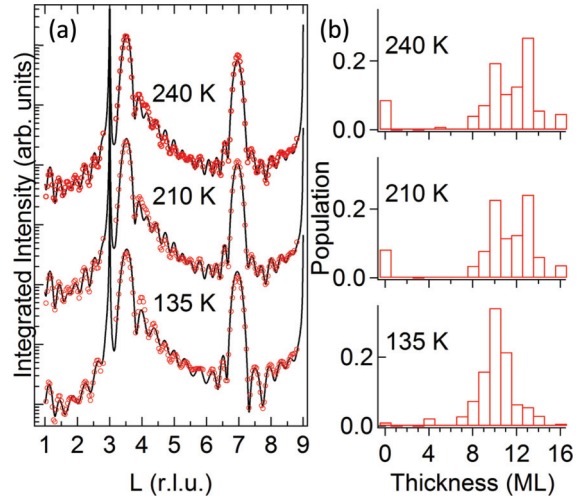


FIG. 5. (Color online) (a) Log plot of the reflectivity (red circles) taken from a 10-ML In film grown on a root-3 surface at 135 K, and from the same film after annealing to 210 and 240 K. The black curves are fits. (b) The corresponding thickness distributions. Note that the thickness distribution appears to shift towards higher thicknesses upon annealing, which is associated with the increased surface area that is not covered by the film (p_0). In other words, the films grow taller at the cost of shrinking area (due to mass conservation).

distribution. The dominant thickness in each case corresponds to the amount deposited, and the width of the distribution is just 2–3 ML. Thus the film grows approximately layer by layer with a roughness about 2–3 ML. Evidently, the deposition temperature is too low for significant interlayer migration of the deposited In atoms, but high enough for in-plane movement within each terrace to form ordered layers. The roughness appears to grow with increasing average thickness of the film. This is consistent with nucleation and island growth on each terrace.

The annealing behavior of a 10 ML film, shown in Fig. 5, indicates that at higher temperatures, In atoms can migrate between different terrace heights to allow the thickness distribution to evolve. The data at 210 and 240 K are similar, suggesting that the system has reached a kind of metastable distribution, which should reflect the energetics of the system. Two preferred thicknesses are observed: 10 and 13 ML. In addition, there is hint of a third preferred thickness at 16 ML.

Our earlier photoemission studies of samples similarly prepared indicate two preferred thicknesses at 4 and 7 ML at low coverages.⁹ Putting the x-ray and photoemission results together, we conclude that the preferred thicknesses are 4, 7, 10, 13, and 16 ML, with the last data point somewhat uncertain. The trilayer sequencing is clear, and this is expected based on the electronic structure of In. While such trilayer oscillation is supported by both the x-ray and photoemission measurements, more morphological measurements, e.g., STM, can be done to further confirm the detailed trilayer sequence and kinetics.

VI. SUMMARY

In films were grown on Si(111)-(7 × 7) and Si(111)-($\sqrt{3} \times \sqrt{3}$)-In surfaces. Significant differences between these systems were observed for growth at 135 K,

which illustrates that the growth behavior can depend strongly on the beginning surface structure. After burial by In films the 7×7 reconstruction was found to persist. The reflectivity data show significant deviation from a multislit interference pattern, and a satisfactory model fit to the data could not be found. The reflectivity data from In films grown on the root-3 surface could be fit well. Growth at 135 K is approximately layer by layer. Annealing results at higher temperatures indicate preferred thicknesses of 10, 13, and possibly 16 ML. Combined with earlier photoemission studies, which show preferred thicknesses of 4 and 7 ML at low coverage, a sequence of preferred thicknesses of 4, 7, 10, 13, and 16 ML could be inferred. The trilayer oscillation period is quite clear

and differs from the bilayer period in Pb films, in accordance with the different electronic structures of the two cases. The In film system is only the second example, after the Pb case, to show significant quantum oscillations over a wide range of film thickness. It provides further evidence that electronic effects affect film stability leading to preferred thicknesses.

ACKNOWLEDGMENTS

This work is supported by the US Department of Energy, Office of Science, Office of Basic Energy Sciences, under Grant No. DE-FG02-07ER46383 (T.-C.C.) and Contract No. DE-AC02-06CH11357 (operations of APS).

-
- ¹T.-C. Chiang, *Science* **306**, 1900 (2004).
²K. Budde, E. Abram, V. Yeh, and M. C. Tringides, *Phys. Rev. B* **61**, R10602 (2000).
³P. Czoschke, H. Hong, L. Basile, and T.-C. Chiang, *Phys. Rev. Lett.* **91**, 226801 (2003).
⁴D. Eom, S. Qin, M. Y. Chou, and C. K. Shih, *Phys. Rev. Lett.* **96**, 027005 (2006).
⁵Y. Guo, Y. Zhang, X. Bao *et al.*, *Science* **306**, 1915 (2004).
⁶H. Hong, C.-M. Wei, M. Y. Chou, Z. Wu, L. Basile, H. Chen, M. Holt, and T.-C. Chiang, *Phys. Rev. Lett.* **90**, 076104 (2003).
⁷M. M. Ozer, Y. Jia, Z. Zhang, J. R. Thompson, and H. H. Weitering, *Science* **316**, 1594 (2007).
⁸W. B. Su, S. H. Chang, W. B. Jian, C. S. Chang, L. J. Chen, and T. T. Tsong, *Phys. Rev. Lett.* **86**, 5116 (2001).
⁹Y. Liu, T. Miller, and T. C. Chiang, *J. Phys.: Condens. Matter* **23**, 365302 (2011).
¹⁰I. B. Altfeder, X. Liang, T. Yamada, D. M. Chen, and V. Narayanamurti, *Phys. Rev. Lett.* **92**, 226404 (2004).
¹¹J. H. Dil, B. Hulsen, T. U. Kampen, P. Kratzer, and K. Horn, *J. Phys.: Condens. Matter* **22**, 135008 (2010).
¹²V. Hnatyuk and M. Stozak, *J. Phys.: Condens. Matter* **19**, 396001 (2007).
¹³M. Jalochocki, *Prog. Surf. Sci.* **48**, 287 (1995).
¹⁴S. Takeda, X. Tong, S. Ino, and S. Hasegawa, *Surf. Sci.* **415**, 264 (1998).
¹⁵J. Chen, M. Hupalo, M. Ji, C. Z. Wang, K. M. Ho, and M. C. Tringides, *Phys. Rev. B* **77**, 233302 (2008).
¹⁶I. K. Robinson, W. K. Waskiewicz, R. T. Tung, and J. Bohr, *Phys. Rev. Lett.* **57**, 2714 (1986).
¹⁷I. K. Robinson and D. J. Tweet, *Rep. Prog. Phys.* **55**, 599 (1992).
¹⁸R. Feidenhans'l, *Surf. Sci. Rep.* **10**, 105 (1989).
¹⁹P. Czoschke, H. Hong, L. Basile, and T.-C. Chiang, *Phys. Rev. Lett.* **93**, 036103 (2004).
²⁰P. Czoschke, H. Hong, L. Basile, and T.-C. Chiang, *Phys. Rev. B* **72**, 075402 (2005).